



HHS Public Access

Author manuscript

Nat Immunol. Author manuscript; available in PMC 2018 March 25.

Published in final edited form as:

Nat Immunol. 2017 November ; 18(11): 1261–1269. doi:10.1038/ni.3849.

Anti-Dengue E-dimer epitope human antibodies have therapeutic activity against Zika virus infection

Estefania Fernandez¹, Wanwisa Dejnirattisai², Bin Cao³, Suzanne M. Scheaffer³, Piyada Supasa², Wiyada Wongwiwat², Prabakaran Esakky³, Andrea Drury³, Juthathip Mongkolsapaya^{2,4}, Kelle H. Moley³, Indira U. Mysorekar^{1,3}, Gavin R. Screaton^{2,*}, and Michael S. Diamond^{1,5,6,7,*}

¹Department of Pathology & Immunology, Washington University School of Medicine, St Louis, MO, USA ²Division of Immunology and Inflammation, Department of Medicine, Hammersmith Campus, Imperial College London, UK ³Department of Obstetrics and Gynecology, Washington University School of Medicine, St Louis, MO, USA ⁴Dengue Hemorrhagic Fever Research Unit, Office for Research and Development, Siriraj Hospital, Faculty of Medicine, Mahidol University, Bangkok, Thailand ⁵Department of Medicine, Washington University School of Medicine, St Louis, MO, USA ⁶Department of Molecular Microbiology, Washington University School of Medicine, St Louis, MO, USA ⁷Andrew M. and Jane M. Bursky Center for Human Immunology and Immunotherapy Programs, Washington University School of Medicine, St Louis, MO, USA

Abstract

The Zika virus (ZIKV) epidemic has resulted in congenital abnormalities in fetuses and neonates. Although some cross-reactive DENV antibodies can enhance ZIKV infection in mice, those recognizing the E-dimer epitope (EDE) can neutralize ZIKV infection in cell culture. We evaluated the therapeutic activity of human EDE monoclonal antibodies (mAbs) for their ability to control ZIKV infection in the brains, testes, placentas, and fetuses of mice. A single dose of EDE1-B10 antibody given three days after infection protected against lethality, reduced ZIKV levels in brains and testes, and preserved sperm counts. In pregnant mice, wild-type or engineered LALA variants of EDE1-B10, which cannot engage Fc- γ receptors, diminished ZIKV burden in maternal and fetal tissues, and protected against fetal demise. As neutralizing EDE antibodies, in

Users may view, print, copy, and download text and data-mine the content in such documents, for the purposes of academic research, subject always to the full Conditions of use: http://www.nature.com/authors/editorial_policies/license.html#terms

*Address correspondence to: Michael S. Diamond, M.D. Ph.D., Departments of Medicine, Molecular Microbiology, and Pathology & Immunology, Washington University School of Medicine, Saint Louis, MO, USA. diamond@wusm.wustl.edu or Gavin R. Screaton, Department of Medicine, Imperial College London, London, United Kingdom. g.screaton@imperial.ac.uk

ACCESSION CODES. None

DATA AVAILABILITY STATEMENT. The data that support the findings of this study are available from the corresponding author upon request.

AUTHOR CONTRIBUTIONS.

E.F., J.M., W.D., S.M.S., B.C., J.M., G.R.S., and M.S.D. designed the experiments. E.F., W.D., S.M.S., B.C., P.S., and W.W. performed the experiments. E.F., J.M., W.D., S.M.S., B.C., P.E., A.D., I.U.M., K.H.M., G.R.S., and M.S.D. analyzed the data. E.F. and M.S.D. wrote the first draft of the paper. All authors participated in editing the final version of the manuscript.

COMPETING FINANCIAL INTEREST STATEMENT

M.S.D. is a consultant for Inbios, Visterra, Aviana, and Sanofi-Pasteur, and is on the Scientific Advisory Boards of Moderna and OvaGene. G.R.S. is on the Vaccine Scientific Advisory Board of GlaxoSmithKline plc.

addition to their established inhibitory effects against DENV, have therapeutic potential against ZIKV, it may be possible to develop therapies that control disease caused by both viruses.

INTRODUCTION

Zika virus (ZIKV) is an arthropod-transmitted, positive-sense RNA virus that is closely related to viruses causing significant human disease such as dengue (DENV), yellow fever (YFV), West Nile (WNV), and Japanese encephalitis (JEV) viruses. Historically, ZIKV infection in humans was associated with a self-limiting mild febrile illness¹. Since its epidemic emergence in 2007, ZIKV infection has become linked to more severe clinical syndromes. For example, infection of pregnant women, particularly during the first trimester, can result in congenital Zika syndrome, which includes microcephaly, neurodevelopmental abnormalities, and fetal demise²⁻⁴. In adults, ZIKV infection is associated with Guillain-Barré syndrome (GBS), an autoimmune disease characterized by ascending paralysis and polyneuropathy^{5,6}.

The ZIKV genome is organized as a single open reading frame that encodes for three structural (capsid (C), pre-membrane/membrane (prM/M), and envelope (E)) and seven non-structural (NS) genes. ZIKV E protein is composed of three domains: a central β -barrel domain (domain I, DI), an extended dimerization domain containing a hydrophobic fusion loop (FL) epitope at the distal end (domain II, DII), and an immunoglobulin-like segment implicated in receptor-binding and entry (domain III, DIII)⁷. In the immature state, prM and E form 60 spiky heterotrimers that protrude from the membrane surface⁸. Maturation during transit through the *trans*-golgi network results in furin-mediated cleavage of prM to M. Upon cleavage, E protein homodimers re-arrange in an anti-parallel orientation forming a herringbone array and a smooth virion surface. The transitions undergone by viral particles expose different epitopes on the E protein that are essential for receptor-binding, entry, and fusion. The E protein also is the primary target for neutralizing antibody responses.

ZIKV strains are classified into two genetic lineages, African and Asian/American. As their neutralization by serum and monoclonal antibodies (mAbs) is quite similar, ZIKV is categorized as a single serotype⁹. Genetic clustering places ZIKV in close relationship to DENV, with a 54–59% amino acid identity in E proteins^{10,11}.

The humoral response to ZIKV infection has been studied by several groups with advances made in our understanding of the epitopes engaged by protective mAbs¹². MAb targeting the cross-reactive DII-FL epitope generally are poorly neutralizing against ZIKV; despite this, passive transfer studies in mice suggest these mAbs can protect to some degree against ZIKV infection, possibly because of ‘virus breathing’ and further exposure of this epitope^{7,13,14}. DII-FL-specific mAbs generated against DENV or ZIKV also have the potential to induce reciprocal antibody dependent enhancement (ADE) of ZIKV or DENV infection in myeloid cells bearing Fc γ receptors (Fc- γ R)^{15,16} and in mice¹⁷. In comparison, strongly neutralizing and protective mouse and human anti-ZIKV mAbs have been described that bind epitopes in DIII (lateral ridge or A-strand^{18,19,20}), across adjacent dimers in DII¹⁹, or to sites in DI²¹. A distinct class of cross-reactive mAbs that engage the DII-FL are the E-dimer epitope (EDE) mAbs. These mAbs were isolated from DENV-infected patients, bind

to an inter-dimer quaternary epitope with contact residues in DI, DII, and DIII, and cross-react with ZIKV^{10,11,16,22}. EDE mAbs are classified by their binding in the context of N-linked glycosylation at position N154 of the E protein. EDE1 mAbs, which bind in the absence of the N-linked glycan, inhibit ZIKV more potently than do EDE2 mAbs^{10,23}.

Studies in mice, non-human primates, and humans have shown that ZIKV can infect and persist in several immune-privileged sites including the eye^{4,24,25}, brain^{24,26,27}, testis^{28,29}, and the placenta^{26,30}. Here, we evaluated the therapeutic activity of EDE1 mAbs in ZIKV infection. Although EDE1-B10 showed protective activity when administered within 5 days of infection, it was less effective at clearing infection from immune-privileged tissues once ZIKV disseminated to these sites. In the context of pregnancy, EDE1 LALA genetic variants, which cannot bind Fc- γ R, protected against ZIKV infection as well as recombinant wild-type mAbs. Our studies suggest it may be possible to develop EDE1 LALA mAb therapeutics that prevent both ZIKV and DENV infection without the possibility for pathological immune enhancement.

RESULTS

Anti-DENV human mAbs inhibit ZIKV infection

Previous studies have established that EDE1-C8 and EDE1-C10 bind to and neutralize ZIKV infection with EC₅₀ values ranging from 9–14 ng/mL^{10,31}. We compared the ability of another EDE1 mAb, EDE1-B10, to neutralize the four serotypes of DENV and the two lineages of ZIKV. EDE1-B10 strongly neutralized DENV serotypes 1, 2, and 3 (EC₅₀ ~ 28–138 ng/mL), with weaker activity against the more distantly related DENV-4 serotype (Fig 1a). When tested against ZIKV strains representing the genetic diversity of the two lineages (African (HD78788) and Asian/American (Brazil PE243), EDE1-B10 had a stronger neutralization profile (EC₅₀ ~ 2–4 ng/mL) than did EDE1-C8 and other published EDE mAbs^{10,23} (Fig 1b). As with other EDE mAbs, EDE1-B10 engages a quaternary epitope on the virion and does not bind monomeric E protein although the epitope is restored on covalently linked E-dimers^{31,32}. Like many other flavivirus antibodies, sub-neutralizing concentrations of EDE mAbs can trigger ADE of Fc- γ R expressing myeloid cells. To prevent possible ADE, we engineered leucine-alanine (LALA) mutations into the Fc region of EDE1-B10 and EDE1-C8; these substitutions disrupted engagement with Fc receptors and prevented ADE but did not change neutralizing activity against ZIKV (Fig 1c, d)³³. Thus, anti-DENV EDE mAbs strongly neutralize ZIKV infection, and LALA variants that do not promote ADE can be generated without a loss of inhibitory activity in cell culture.

EDE1 mAb therapy controls ZIKV infection

We tested EDE human mAbs for their ability to protect mice against ZIKV-induced lethality when administered as a post-exposure therapy. To create a lethal challenge model in 4 to 5 week-old C57BL/6 mice, we passively transferred a blocking anti-Ifnar1 antibody one day prior to infection with 10³ focus-forming units (FFU) of a mouse-adapted African strain of ZIKV (ZIKV-Dakar)^{18,19}. Mice then were treated with a single dose of EDE1-B10, EDE1-C8, EDE2-A11 (EC₅₀ of 69–125 ng/ml)¹⁰ or an isotype control mAb (Flu 28C) at day +1 (100 μ g), +3 (250 μ g), or +5 (250 μ g) after infection, and weight and survival were

monitored for 21 days (Fig 2a, Supplementary Fig 1). Mice treated with EDE1-B10, EDE1-C8, or EDE2-A11 were protected against lethality when treated at one or three days after infection. Furthermore, EDE1-B10 treatment at 5 days after infection resulted in partial protection against lethality and weight loss. Given the greater neutralization activity of EDE1-B10 *in vitro* and robust protection against lethality, most subsequent *in vivo* studies were performed only with EDE1-B10.

As a first step toward determining how EDE1 mAbs protect against disease, we defined the kinetics of viral dissemination at the tissues of interest. Within two days of infection, ZIKV RNA was readily detectable in the serum (Fig 2b, 1.7×10^5 FFU equivalents per mL), brain (Fig 2c, 3.5×10^3 FFU equivalents per g), testis (Fig 2d, 4.8×10^3 FFU equivalents per g), epididymis (Fig 2e, 5.0×10^2 FFU equivalents per g), and eye (Fig 2f, 8.8×10^2 FFU equivalents per g). At the last time point assessed (day +5), viral titers were still increasing in these organs.

We then evaluated the efficacy of EDE1-B10 therapy on the control of ZIKV infection at different immune privileged sites during the acute and persistent phases. Adult C57BL/6 male mice were pre-treated with anti-Ifnar1 blocking antibody and inoculated with 10^5 FFU of mouse-adapted ZIKV-Dakar. Mice then were administered a single dose of EDE1-B10 or an isotype control mAb at day +1 (100 μ g), +3 (250 μ g), or +5 (250 μ g) after infection, and viral RNA levels were assessed at day +5 (acute phase) or day +21 (persistent phase) after infection. Treatment at day +1 decreased the levels of ZIKV RNA circulating in serum at day +5 (52-fold, $P < 0.001$; Fig 2g). Similarly, EDE1-B10 therapy at day +1 reduced viral RNA levels in the brain (1,760-fold and 42-fold, $P < 0.001$), testis (1,650-fold and 312-fold, $P < 0.001$), and epididymis (4,780-fold and 206-fold, $P < 0.001$) at day +5 (Fig 2h–j) and day +21 (Fig 2l–n), respectively, compared to the isotype-control mAb. Whereas reduced levels were observed in the eye at day +5 after EDE1-B10 therapy at day +1 (1,550-fold, $P < 0.001$; Fig 2k), ZIKV RNA levels were low at day +21 in EDE1-B10 and isotype control mAb groups suggesting clearance occurred independently of mAb treatment (Fig 2o).

In another set of experiments, we treated mice with EDE1-B10 at D+3 and evaluated effects on tissue viral burden at D+5 and D+21. Treatment at day +3 with EDE1-B10 had less effect on viral RNA levels at day +5 with smaller reductions observed in serum (4-fold, $P < 0.05$), the brain (9-fold, $P < 0.001$), testis (3-fold, $P > 0.05$), epididymis (116-fold, $P < 0.001$), and eye (3-fold, $P < 0.05$) (Fig 2g–k). In comparison, EDE1-B10 treatment at D+3 resulted in decreased ZIKV RNA levels in the testis (62-fold, $P < 0.05$) and epididymis (1,800-fold, $P < 0.05$) at D+21 although levels in the brain were not affected (Fig 2l–n).

Finally, we evaluated EDE1-B10 therapy at D+5 for its effect on viral burden at D+21. However, treatment with EDE1-B10 beginning D+5 after infection failed to inhibit ZIKV RNA levels at day +21 in any of the sites tested. To begin to define why EDE1-B10 protected at some sites but not others, we measured mAb levels in tissues at D+5 after therapy was initiated at D+1 or D+3 (Supplementary Fig 2). Although levels of EDE1-B10 in serum at D+5 were relatively equivalent, levels in the brain and testis were lower ($P < 0.01$) when therapy was started at D+1 than D+3. This may reflect the diminished systemic viral burden associated with D+1 treatment, which we speculate limits pro-inflammatory

immune responses that compromise the blood-brain-barrier and blood-testis barrier function and allows EDE1-B10 access. Notably, lower levels of EDE1-B10 penetrated into the eye at D+5 regardless of day of treatment, which may be due to a less permeable blood-retinal barrier³⁴. As treatment at D+5 failed to reduce viral RNA levels at D+21, once immune-privileged sites are seeded, it may be difficult to accumulate sufficient levels of EDE1-B10 mAb to control or clear infection. In summary, these experiments show a narrow window after infection where treatment with EDE1-B10 mAb reduced ZIKV RNA levels in some but not other immune privileged sites, once viral seeding had occurred.

To corroborate the protective effects observed with EDE1-B10 therapy, we evaluated ZIKV infection in the male reproductive tract at day +21 using RNA *in situ* hybridization (ISH). RNA ISH confirmed the absence of ZIKV RNA in the testis and epididymis of mice treated with EDE1-B10 at day +1 after infection and showed reduced viral RNA levels when treatment was initiated at day +3 after infection (Fig 3a, Supplementary Fig 3); in comparison, isotype control mAb treated animals had high viral RNA levels as reported for untreated, infected mice²⁸. Treatment at day +1 or day +3 with EDE1-B10 also protected against ZIKV-induced inflammation and damage to the seminiferous tubules that was seen with the isotype control mAb (Fig 3b, Supplementary Fig 3) and described previously^{28,29}. In contrast, treatment beginning at day +5 minimally protected against ZIKV infection or injury. We also evaluated the functional effect of EDE1-B10 in the testis by computer-assisted sperm analysis. Whereas isotype-control mAb treated ZIKV-infected mice showed low numbers of motile sperm, treatment with EDE1-B10 at days 1 or 3 but not 5 resulted in higher levels (16 and 100-fold respectively, $P < 0.001$) at day +21 (Fig 3c), which approached those from age-matched uninfected male mice. These data suggest that EDE1-B10 can reduce viral persistence in select immune privileged sites (e.g., brain and testis) and protect against tissue injury when administered within a few days of infection.

EDE1-B10 therapy in maternal and fetal tissues

Placental damage and fetal infection and injury occurs in pregnant mice deficient in type I IFN signaling after ZIKV infection^{25,30,35,36}. To assess the protective ability of EDE1-B10 during pregnancy, we mated *Ifnar1*^{-/-} dams with wild-type C57BL/6 sires and on embryonic day 6.5 (E6.5), inoculated them subcutaneously with a Brazilian ZIKV strain (Paraiba 2015)^{19,35}. One day after infection (E7.5), we administered a single 250 μ g dose of EDE1-B10 or an isotype-control mAb and monitored effects on the *Ifnar1*^{-/-} dam and the *Ifnar1*^{+/-} placenta and fetus. Seven days after ZIKV inoculation (E13.5), the isotype-control mAb treated group sustained a 90% rate of fetal demise compared to a 10% rate in the dams treated with EDE1-B10 ($P < 0.0001$) (Fig 4a, *left*). Histological analysis confirmed that the fetal demise caused by ZIKV infection was prevented with EDE1-B10 therapy (Fig 4a, *right*). Consistent with these data, EDE1-B10 treatment at day +1 reduced viral RNA burden in the maternal serum (~71-fold, $P < 0.01$) and brain (~39,000-fold, $P < 0.05$) at day +7 after infection (Fig 4b and c). Analysis of the placentas by ISH showed ZIKV RNA in the maternal decidua and the junctional layer of the placenta in the isotype-control mAb treated mice; in contrast, viral RNA staining was not observed in dams treated with EDE1-B10 (Fig 4d). Histological analysis after ZIKV infection showed reductions in the size of the labyrinth

layer of the placenta in isotype-treated dams, which was reversed with EDE1-B10 treatment at day +1 after infection (Fig 4e).

The extent of fetal demise after ZIKV infection of *Ifnar1*^{-/-} dams precluded virological assessment of EDE1-B10 protection in the fetus. To obtain such data, we utilized a second model of ZIKV infection in pregnancy with an acquired deficiency of type I IFN signaling^{19,35}. WT females mated with WT males were treated with anti-*Ifnar1* blocking mAb at E5.5. One day later (E6.5), dams were inoculated subcutaneously with mouse-adapted ZIKV-Dakar, and one (E7.5) or three (E9.5) days later treated with EDE1-B10 or an isotype-control mAb. Treatment of pregnant dams at day +1 EDE1-B10 reduced viral RNA in the maternal serum (~240-fold, $P < 0.001$) and brain (~3,000-fold, $P < 0.05$) from the level in isotype-control mAb treated dams (Fig 5a, b). When treatment was initiated at day +1, we observed markedly reduced if not abolished ZIKV RNA levels in the placenta and fetal head (660,000-fold and 4,900-fold respectively, $P < 0.0001$) of EDE1-B10 treated dams relative to the isotype control (Fig 5c, d). Treatment of dams with EDE1-B10 at day +3 also reduced ZIKV RNA levels in the maternal serum (22-fold, $P < 0.05$) and brain (114-fold, $P < 0.001$) (Fig 5a, b). Although ZIKV levels in the placenta (23-fold, $P < 0.0001$) and fetal head (19-fold, $P < 0.0001$) were lower in the EDE1-B10-treated groups, therapy at this time point did not prevent virus seeding (Fig 5c, d).

We next evaluated whether antibody effector functions were required for EDE1-B10 mediated protection. We generated a mutant version of the EDE1-B10 mAb (LALA variant³³) that was unable to bind to Fc- γ R and promote ADE (Fig 1c) and tested its efficacy *in vivo* during pregnancy. Like therapy with the recombinant wild-type EDE1-B10 mAb, treatment of dams with EDE1-B10 LALA at day +1 after infection resulted in reduced viral RNA levels in the maternal serum (240-fold, $P < 0.01$), maternal brain (3,000-fold, $P < 0.05$), placenta (633,000-fold, $P < 0.0001$), and fetal head (4,600-fold, $P < 0.0001$) (Fig 5a–d). Analogous experiments with paired recombinant wild-type and LALA EDE1-C8 mAbs yielded similar results (Supplementary Fig 4). Thus, *in utero* protection mediated by EDE1 mAbs occurs independently of Fc effector functions and likely is mediated by direct virus neutralization. The Fc- γ R-binding mutant mAbs could be safer immunotherapies, as they lack the potential to mediate ADE and immunopathogenesis.

To corroborate the protective effects in the placenta, we analyzed tissue sections for virus infection and tissue injury. RNA ISH of placentas from dams treated at day +1 showed a virtual absence of ZIKV-infected cells in the decidua and placenta, and animals treated at day +3 also showed reduced viral RNA staining compared to isotype-control treated dams (Fig. 5e). Histological measurements of placental layers showed that treatment at day +1 but not day +3 with EDE1-B10 restored the area and width of the junctional area, the total placental area, and overall fetal size (Fig. 5f–i) compared to the isotype-control mAb. These data confirm a narrow therapeutic window for EDE1-B10 for preventing ZIKV infection and injury to the developing placenta and fetus.

Sexual transmission is an established route of ZIKV infection^{37–42}. Male-to-female transmission of ZIKV has been modeled in pregnant mice through direct intravaginal inoculation of virus³⁰. Although recent vaccine studies indicate that adaptive immune

responses can protect against *in utero* transmission if ZIKV is inoculated subcutaneously⁴³, no study has shown this in the context of vaginal transmission. We assessed whether administration of EDE1-B10 through a peripheral route could prevent *in utero* transmission following intravaginal inoculation of ZIKV. WT dams mated with WT sires were treated with anti-Ifnar1 blocking mAb and a single 250 µg dose of EDE1-B10 or isotype-control mAb at E5.5. At E6.5, dams were inoculated via intravaginal route with mouse-adapted ZIKV-Dakar. On E7.5, dams were given a second dose of anti-Ifnar1 blocking mAb. At day E13.5, we determined viral RNA burden in maternal and fetal tissues, including those of the female reproductive tract. Treatment with EDE1-B10 reduced ZIKV RNA levels in the maternal serum (427-fold, $P < 0.05$) and brain (45,490-fold, $P < 0.01$) (Fig 6a, b) compared to isotype control mAb-treated mice. In EDE1-B10-treated dams, ZIKV RNA levels were diminished in all female reproductive tract tissues including the vagina (106,840-fold, $P < 0.01$), cervix (12,450-fold, $P < 0.01$), and ovaries (341,300-fold, $P < 0.01$) (Fig 6c–e). As EDE1-B10 also reduced ZIKV RNA levels in the placenta (1,725,600-fold, $P < 0.0001$) and fetal head (3,020-fold, $P < 0.0001$) (Fig 6f and g), circulating neutralizing antibodies can prevent transvaginal transmission of ZIKV to the placenta and fetus. Consistent with these data, staining by ISH showed a virtual absence of ZIKV RNA in the placenta and decidua of EDE1-B10 treated compared to isotype-control treated dams (Fig 6h). Overall, these experiments establish that EDE1-B10 therapy can protect against ZIKV infection and transmission to the fetus after subcutaneous or intravaginal inoculation routes.

DISCUSSION

A primary goal of this study was to identify human mAbs that could potentially neutralize ZIKV and provide post-exposure protection *in vivo*, including reduction of infection in key immune privileged sites. Prior studies showed that E-dimer epitope (EDE) mAbs, isolated from DENV-infected subjects, can neutralize DENV and ZIKV *in vitro*^{10,11} and protect against ZIKV lethality *in vivo* when administered as prophylaxis²². Studies with more ZIKV-specific human mAbs that do not cross-react to DENV also have demonstrated post-exposure therapeutic activity in lethality models in mice^{17,19–21}. Based on *in vitro* neutralization studies, we defined EDE1-B10 as a candidate because of its strongly inhibitory activity against three strains encompassing the genetic diversity of ZIKV as well as its neutralizing activity against DENV-1, DENV-2, and DENV-3. Of interest, EDE1-B10 failed to bind or neutralize DENV-4 efficiently; this phenotype was similar to that described for cross-reactive mouse anti-DENV mAbs that react with the DII-FL epitope⁴⁴.

We compared EDE1-B10 with previously published EDE mAbs^{10,11}, EDE1-C8 and EDE2-A11, for their post-exposure therapeutic activity against lethal ZIKV challenge. Although all three EDE mAbs completely protected when given 3 days after ZIKV inoculation, EDE1-B10 also reduced lethality when administered 5 days after infection. The combination of increased neutralizing and protective activity led us to select EDE1-B10 for subsequent studies. We assessed how EDE1-B10 functioned at immune privileged sites, which were seeded within two days of virus inoculation. ZIKV replication in immune sanctuary sites may contribute to its persistence in human and animal body fluids including semen, urine, and saliva^{28,29,45,46}. During the acute phase of infection, EDE1-B10 markedly reduced viral RNA in multiple immune privileged sites when administered at day +1. However, the

reductions were lower in magnitude when EDE1-B10 was initiated at day +3. Correspondingly, persistence of ZIKV RNA at day 21 was markedly diminished at most immune privileged sites when therapy was initiated at day +1. However, when therapy was started at day +3, viral RNA persisted at day +21 at several immune privileged sites (eye, brain, and testis). Thus, the likely protective role of the EDE1 mAbs is to limit ZIKV dissemination, with antibody-mediated clearance of already infected immune privileged sites being substantially less efficient. Consistent with this observation, protection of the placenta and fetuses by wild-type and LALA variants of EDE1-B10 and EDE1-C8 was equivalent in the dam infection model and was not dependent on Fc-dependent interactions. These results contrast with HIV³³, Ebola virus⁴⁷, influenza A virus⁴⁸, and respiratory syncytial virus⁴⁹ studies where antibody effector functions enhanced protection. Fc effector functions may contribute to antibody-mediated protection of these viruses because unlike ZIKV, they bud from the plasma membrane and express structural proteins on the cell surface, which can serve as targets of antibody-dependent cellular cytotoxicity.

Sexual transmission is an established route of ZIKV spread and of concern to those within and traveling to endemic regions, particularly for those of child-bearing age. Our study shows that systemic mAb administration can protect against intravaginal transmission of ZIKV infection in the context of pregnancy. This observation is relevant since macaque studies suggest that ZIKV replication in the female reproductive tract precedes infection of peripheral organ tissues that contribute to viremia⁵⁰. Our passive antibody transfer experiments in mice suggest that ZIKV vaccines that induce robust neutralizing antibody responses and protect against *in utero* transmission after subcutaneous virus challenge⁴³ may also prevent sexual transmission.

ZIKV epidemics in the Americas now occur in DENV endemic regions. Cross-reactive antibodies against ZIKV and DENV could protect or mediate pathogenesis⁵¹ depending on the stoichiometry of binding and mechanism of action³². Our pre-clinical studies with LALA variants of EDE1-B10 and EDE1-C8 provide a first step toward developing a safe and effective therapeutic antibody against both ZIKV and DENV, without the possibility for pathogenic immune enhancement. Nonetheless, as the extent to which these findings in mice translate to humans remains unclear, protection studies with EDE1 mAbs in non-human primate models of ZIKV infection in pregnancy are warranted. If these data are promising, human clinical trials will be required to show efficacy. The design of such trials will be challenging given the ephemeral nature of mosquito-transmitted virus epidemics in a given locale and the absolute need for safety in the context of transmission studies with pregnant women.

Online methods

Viruses

ZIKV-Brazil (Paraiba, 2015) was provided by S. Whitehead (National Institute of Health) and originally obtained from P.F.C. Vasconcelos (Instituto Evandro Chagas). Mouse-adapted ZIKV-Dakar 41519 was passaged twice *in vivo* in *Rag1*^{-/-} mice (M.J.G. and M.S.D., unpublished data) and grown in Vero cells. DENV-2 strain D2S20 was obtained (gift of S. Shrestha) and grown in C6/36 *Aedes albopictus* cell line. Primary isolates of

DENV-1 (02-0435; GenBank accession No. JQ740878), DENV-3 (2-1969; GenBank accession No. JQ740881) and DENV-4 (1-0093; GenBank accession No. JQ740883) were obtained from DENV-infected patients in Thailand (provided by P. Malasit and S. Noisakran). DENV-2 (DF-699; GenBank accession No. FM210221) was isolated from a patient in Vietnam (provided by C. Simmons). DENV-2 strain 16681 was a gift from AFRIMS. Additional ZIKV strains from Brazil (PE243, provided by A. Kohl, R.F. de Oliveira Freitas and L.J. Pena) and Africa (HD78788, provided by A. Sakuntabhai) were used for neutralization assays. Virus stocks were titered by focus-forming assay (FFA) on Vero cells as described⁵².

Antibody generation

Activated antibody secreting cells (CD19⁺, CD3⁻, CD20^{lo} or CD20⁻, CD27^{hi} and CD138^{hi}) were sorted by flow cytometry. To amplify VH and VL genes, one step RT-PCR (Qiagen) and nested PCR (Qiagen) were performed. The nested PCR products were cloned into expression vectors encoding the human IgG1 constant region or the LALA variant IgG1 (leucine to alanine substitutions at positions 116 and 117) for the VH gene and the human Ig κ constant region for the VL gene. Plasmids encoding heavy and light chains were co-transfected into HEK 293T cells by the polyethylenimine method (Sigma). Wild-type and LALA variant IgG1 were purified by Protein G plus/Protein A agarose (Merck).

Neutralization assays

Serial dilutions of mAbs were incubated with 10² FFU of the different DENV serotypes or ZIKV strains for 1 h at 37 °C. The mAb–virus complexes were added to Vero cell monolayers in 96-well plates for 2 h at 37 °C. Subsequently, cells were overlaid with 1.5% (w/v) carboxymethyl cellulose in Modified Eagle Medium (MEM) supplemented with 3% heat-inactivated FBS. Plates were fixed 72 h later for DENV and 48 h later for ZIKV with 4% PFA in PBS for 10 min and permeabilized with 2% Triton X-100 in PBS for 10 min at room temperature. Plates were stained with mAb 4G2 supernatant (cross-reactive mouse anti-flavivirus mAb targeting the FL epitope) at 37 °C for 1 h followed by peroxidase-conjugated goat anti-mouse immunoglobulin (Sigma) at a dilution of 1:1,000 in 0.05% Tween-PBS and incubated at 37 °C for 1 h. Foci were visualized by adding DAB substrate (Sigma) at a concentration 0.6 mg/ml.

ADE assay

Serial dilutions of mAbs were incubated with virus at an MOI of 5 at 37°C for 1 h before adding to U937 myelomonocytic leukemia cells. After 24 h of incubation at 37°C, cells were harvested and washed with FACS buffer (2% FBS, 0.5% BSA and 0.1% NaN₃ in PBS). Cells were fixed and permeabilized for 10 min at room temperature with 4% PFA in PBS and 0.5% (w/v) saponin in FACS buffer, respectively. Finally, cells were stained with Alexa Fluor 647 conjugated 4G2 mAb and analyzed using a BD LSRFORTESSA X-20 flow cytometer.

Mouse experiments

Animal studies were carried in accordance with the recommendations of the Guide for the Care and Use of Laboratory Animals of the National Institutes of Health, and were approved by the Institutional Animal Care and Use Committee at the Washington University School of Medicine (Assurance number A3381-01). Mice were inoculated with ZIKV after induction of anesthesia using ketamine hydrochloride and xylazine, and all efforts were made to minimize pain and suffering. Antibody protection studies were performed in the following models: a lethal challenge model in which WT C57BL/6 mice (4–5 week-old, Jackson Laboratories) were administered 2 mg anti-Ifnar1 mAb (MAR1-5A3, Leinco Technologies) by an intraperitoneal injection one day prior to inoculation with 10^3 FFU of mouse-adapted ZIKV-Dakar by subcutaneous route in the footpad. Cross-reactive EDE mAbs (EDE1-C8, EDE1-B10, or EDE2-A11) or isotype control (Flu 28C) human mAbs were administered by intraperitoneal route as a single dose at day +1 (100 μ g, 5 mg/kg), day +3 (250 μ g, 12.5 mg/kg), or day +5 (250 μ g, 12.5 mg/kg) after infection. All animals were monitored for lethality for 21 days. Time course studies in which WT C57BL/6 mice (8–9 week-old, Jackson Laboratories) were treated with 0.5 mg of anti-Ifnar1 mAb by intraperitoneal injection one day prior to inoculation with 10^5 FFU of mouse-adapted ZIKV-Dakar by subcutaneous route. Animals were euthanized at day +1, day +2, day +3, day +4, or day +5 after infection. Acute phase mAb protection studies in which WT C57BL/6 mice (8–9 week-old, Jackson Laboratories) were treated with 0.5 mg anti-Ifnar1 mAb by intraperitoneal injection one day prior to inoculation with 10^5 FFU of mouse-adapted ZIKV-Dakar by subcutaneous route. Cross-reactive EDE1-B10 or an isotype control mAb (Flu 28C) was administered by intraperitoneal route as a single dose at day +1 or day +3 after infection as described above. All animals were euthanized at day +5, and tissues were harvested following extensive perfusion with PBS. Persistence phase mAb protection studies in which WT C57BL/6 mice (8–9 week-old, Jackson Laboratories) were treated with 0.5 mg anti-Ifnar1 mAb by intraperitoneal injection one day prior to inoculation with 10^5 FFU of mouse-adapted ZIKV-Dakar by subcutaneous route. Cross-reactive EDE1-B10 or an isotype control mAb (Flu 28C) was administered by intraperitoneal route as a single dose at day +1, day +3, or day +5 as described above. All animals were euthanized at day 21, and tissues were harvested.

Pregnancy studies in which WT C57BL/6 mice were bred in a specific-pathogen-free facility at Washington University School of Medicine. In some experiments, *Ifnar1*^{-/-} females and wild-type males were mated. At embryonic day E6.5, dams were inoculated with 10^3 FFU of ZIKV-Brazil (Paraiba 2015) by subcutaneous route. At E7.5, dams were treated by intraperitoneal route with a single 250 μ g dose of EDE1-B10 or an isotype control mAb. In another series of experiments, WT female and male mice were mated. At E5.5, dams were treated with 1 mg of anti-Ifnar1 by intraperitoneal route. At E6.5, mice were inoculated with 10^3 FFU mouse-adapted ZIKV-Dakar by subcutaneous route. At E7.5, all mice received a second 1 mg dose of anti-Ifnar1 mAb through an intraperitoneal route. For treatment, mice received a single 250 μ g dose of EDE1-B10, EDE1-B10 LALA, EDE1-C8, EDE1-C8 LALA, or isotype-control mAb by intraperitoneal route on E7.5 (day +1) or E9.5 (day +3, excluding the LALA mutants). All animals were euthanized at E13.5, and placentas, fetuses, and maternal tissues were collected. Finally, in another series of studies, WT female and male mice were mated. At E5.5, dams were treated via an intraperitoneal route with 1.5 mg

of anti-Ifnar1 and a single 250 µg dose of EDE1-B10 or isotype control mAb. At E6.5, mice were inoculated with 10⁵ FFU mouse-adapted ZIKV-Dakar by intravaginal route in 10 µl following swabbing. At E7.5, all mice received a second 1 mg dose of anti-Ifnar1. At E13.5, mice were euthanized, and placentas, fetuses, and maternal tissues were collected.

Measurement of viral burden

ZIKV-infected tissues were weighed and homogenized with stainless steel beads in a Bullet Blender instrument (Next Advance) in 600 µl (brain) or 200 µl (testis, epididymis, eye, vagina, cervix, and ovaries) of PBS. Samples were clarified by centrifugation (2,000 × *g* for 10 min). All homogenized tissues from infected animals were stored at -80°C. Tissue samples and serum from ZIKV-infected mice were extracted with RNeasy 96 Kit (tissues) or Viral RNA Mini kit (serum) (Qiagen). ZIKV RNA levels were determined by Taqman one-step quantitative reverse transcriptase PCR (qRT-PCR) on an ABI7500 Fast Instrument using published primers and conditions⁵³. Viral burden was expressed on a log₁₀ scale as viral RNA equivalents per g or ml after comparison with a standard curve produced using serial tenfold dilutions of ZIKV RNA.

Measurement of EDE1-B10 in tissues

ZIKV-infected tissues from perfused mice were weighed and homogenized with stainless steel beads in a Bullet Blender instrument (Next Advance) in 600 µl (brain) or 300 µl (testis, epididymis, and eye) of PBS. Samples were clarified by centrifugation (2,000 × *g* for 10 min). All homogenized tissues from infected animals were stored at -80°C. Flat-bottom 96-well MaxiSorp (ThermoFisher) plates were coated with goat anti-human (IgG H+L chain) antibody (KPL) and then blocked with PBS + 2% BSA (Sigma) for 1 h at 37 °C. Tissue homogenates were diluted in PBS + 2% BSA and incubated for 1 h at 4°C. Plates were washed six times and then incubated with AffiniPure horseradish peroxidase conjugated goat-anti human IgG (Jackson Immuno) for 1 h at 4 °C and developed with TMB-substrate. The reaction was stopped by addition of 2 N H₂SO₄, and emission (450 nm) was read using a TriStar LB 941 reader (Berthold Technologies). EDE1-B10 levels are shown in µg/ml after comparison with a standard curve and logistic regression produced using serial threefold dilutions of EDE1-B10 in corresponding naïve tissue homogenate tissues.

Viral RNA *in situ* hybridization

RNA *in situ* hybridization was performed with RNAscope 2.5 (Advanced Cell Diagnostics) according to the manufacturer's instructions. PFA-fixed paraffin embedded placental sections were deparaffinized by incubation for 60 min at 60°C. Endogenous peroxidases were quenched with H₂O₂ for 10 min at room temperature. Slides were boiled for 15 min in RNAscope Target Retrieval Reagent and incubated for 30 min in RNAscope Protease Plus before probe hybridization. The probe targeting ZIKV RNA was designed and synthesized by Advanced Cell Diagnostics (catalogue number 467771). Negative control (targeting bacterial gene *dapB*) probe was also obtained from Advanced Cell Diagnostics (catalogue number 310043). Tissues were counterstained with Gill's haematoxylin and visualized with standard bright-field microscopy.

Histology

Testis and epididymis were collected and fixed overnight in 4% paraformaldehyde (PFA) in PBS. Subsequently, 5- μ m-thick sections from EDE1-B10 or isotype-control mAb treated mice were processed for histology by haematoxylin and eosin (H & E) staining. Collected placentas were fixed in 10% neutral buffered formalin at room temperature and embedded in paraffin. Placentas were sectioned and stained with H & E to assess morphology. Surface area and thickness of placenta and different layers were measured using Image J software.

Computer-assisted sperm analysis

Mature sperm from the cauda epididymis of EDE1-B10 or isotype-control mAb treated mice at day +21 after infection were collected immediately after euthanasia as reported⁵⁴. The sperm suspension, in vitrofert medium (Cook Medical), was analyzed using the HTM-IVOS Vs12 integrated visual optical system motility analyzer (Hamilton-Thorne Research) as described previously⁵⁵. All measurements of motile sperm were made within 60 min of dissection of the cauda epididymis.

Statistical analysis

All data were analyzed with GraphPad Prism software. Kaplan-Meier survival curves were analyzed by the log-rank test. Viral burden and viremia were analyzed by the Mann-Whitney test. Motile sperm and placental and fetal measurements were analyzed by ANOVA using either a Kruskal-Wallis or Holm-Sidak's test with a multiple comparisons correction. Fetal outcome was assessed by Fisher's exact test. Additional detail can be found in the Life Sciences Reporting Summary.

Supplementary Material

Refer to Web version on PubMed Central for supplementary material.

Acknowledgments

This work was supported by grants from the NIH (R01 AI073755 and R01 AI127828 to M.S.D; R01 HD091218 to I.U.M and M.S.D.; T32 AI007163 to E.F.), Wellcome Trust to G.R.S., MRC-NEWTON UK to J.M, and The National Institute for Health Research Biomedical Research Centre funding scheme UK. The authors thank Haina Shin for advice on the intravaginal infection experiments.

References

1. Weaver SC, et al. Zika virus: History, emergence, biology, and prospects for control. *Antiviral Res.* 2016; 130:69–80. [PubMed: 26996139]
2. Brasil P, et al. Zika Virus Infection in Pregnant Women in Rio de Janeiro. *N Engl J Med.* 2016; 375:2321–2334. [PubMed: 26943629]
3. Schaub B, et al. Analysis of blood from Zika virus-infected fetuses: a prospective case series. 2017; 3099:26–28.
4. Honein MA, et al. Birth Defects Among Fetuses and Infants of US Women With Evidence of Possible Zika Virus Infection During Pregnancy. *Jama.* 2016; 30333:59–68.
5. Cao-Lormeau VM, et al. Guillain-Barré Syndrome outbreak associated with Zika virus infection in French Polynesia: a case-control study. *Lancet.* 2016; 387:1531–1539. [PubMed: 26948433]
6. Parra B, et al. Guillain- Barre Syndrome Associated with Zika Virus Infection in Colombia. *N Engl J Med.* 2016; 373:1513–1523.

7. Dai L, et al. Structures of the Zika Virus Envelope Protein and Its Complex with a Flavivirus Broadly Protective Antibody. *Cell Host Microbe*. 2016; 19:696–704. [PubMed: 27158114]
8. Kuhn RJ, et al. Structure of dengue virus: Implications for flavivirus organization, maturation, and fusion. *Cell*. 2002; 108:717–725. [PubMed: 11893341]
9. Dowd KA, et al. Broadly Neutralizing Activity of Zika Virus-Immune Sera Identifies a Single Viral Serotype. *Nature*. 2016; 11:1485–91.
10. Barba-Spaeth G, et al. Structural basis of potent Zika–dengue virus antibody cross-neutralization. *Nature*. 2016; 536:48–53. [PubMed: 27338953]
11. Dejnirattisai W, et al. A new class of highly potent, broadly neutralizing antibodies isolated from viremic patients infected with dengue virus. *Nat Immunol*. 2014; 16:170–177. [PubMed: 25501631]
12. Fernandez E, Diamond MS. Vaccination strategies against Zika virus. *Curr Opin Virol*. 2017; 23:59–67. [PubMed: 28432975]
13. Nelson S, et al. Maturation of West Nile Virus Modulates Sensitivity to Antibody-Mediated Neutralization. *PLoS Pathog*. 2008; 4:e1000060. [PubMed: 18464894]
14. Kam Y-W, et al. Cross-reactive dengue human monoclonal antibody prevents severe pathologies and death from Zika virus infections. *JCI Insight*. 2017; 2
15. Halstead SB, Mahalingam S, Marovich MA, Ubol S, Mosser DM. Intrinsic antibody-dependent enhancement of microbial infection in macrophages: disease regulation by immune complexes. *Lancet Infect Dis*. 2010; 10:712–722. [PubMed: 20883967]
16. Dejnirattisai W, et al. Dengue virus sero-cross-reactivity drives antibody-dependent enhancement of infection with zika virus. *Nat Immunol*. 2016; 17:1102–1108. [PubMed: 27339099]
17. Stettler K, et al. Specificity, cross-reactivity, and function of antibodies elicited by Zika virus infection. *Science (80-)*. 2016; 353:823–826.
18. Zhao H, et al. Structural Basis of Zika Virus-Specific Antibody Protection. *Cell*. 2016; 166:1016–1027. [PubMed: 27475895]
19. Sapparapu G, et al. Neutralizing human antibodies prevent Zika virus replication and fetal disease in mice. *Nature*. 2016; 540:443–447. [PubMed: 27819683]
20. Robbiani DF, et al. Recurrent Potent Human Neutralizing Antibodies to Zika Virus in Brazil and Mexico. *Cell*. 2017; 169:597–609.e11. [PubMed: 28475892]
21. Wang Q, et al. Molecular determinants of human neutralizing antibodies isolated from a patient infected with Zika virus. *Sci Transl Med*. 2016; 8:369ra179.
22. Swanstrom JA, et al. Dengue Virus Envelope Dimer Epitope Monoclonal Antibodies Isolated from Dengue Patients Are Protective against Zika Virus. *MBio*. 2016; 7:e01123–16. [PubMed: 27435464]
23. Dejnirattisai W, et al. Dengue virus sero-cross-reactivity drives antibody- dependent enhancement of infection with zika virus. *Nat Publ Gr*. 2016; 17:1102–1108.
24. Hirsch AJ, et al. Zika Virus infection of rhesus macaques leads to viral persistence in multiple tissues. *PLoS Pathog*. 2017; 13
25. Miner JJ, et al. Zika Virus Infection in Mice Causes Panuveitis with Shedding of Virus in Tears. *Cell Rep*. 2016; 16:3208–3218. [PubMed: 27612415]
26. Bhatnagar J, et al. Zika virus RNA replication and persistence in brain and placental tissue. *Emerg Infect Dis*. 2017; 23:405–414. [PubMed: 27959260]
27. Aid M, et al. Zika Virus Persistence in the Central Nervous System and Lymph Nodes of Rhesus Monkeys. *Cell*. 2017; 169:610–620.e14. [PubMed: 28457610]
28. Govero J, et al. Zika virus infection damages the testes in mice. *Nature*. 2016; 540:438–442. [PubMed: 27798603]
29. Ma W, et al. Zika Virus Causes Testis Damage and Leads to Male Infertility in Mice. *Cell*. 2016; 167:1511–1524.e10. [PubMed: 27884405]
30. Yockey LJ, et al. Vaginal Exposure to Zika Virus during Pregnancy Leads to Fetal Brain Infection. *Cell*. 2016; 166:1247–1256.e4. [PubMed: 27565347]
31. Rouvinski A, et al. Covalently linked dengue virus envelope glycoprotein dimers reduce exposure of the immunodominant fusion loop epitope. *Nat Commun*. 2017; 8:15411. [PubMed: 28534525]

32. Pierson TC, Diamond MS. A game of numbers: The stoichiometry of antibody-mediated neutralization of flavivirus infection. *Progress in Molecular Biology and Translational Science*. 2015; 129:141–166. [PubMed: 25595803]
33. Hessel AJ, et al. Fc receptor but not complement binding is important in antibody protection against HIV. *Nature*. 2007; 449:101–104. [PubMed: 17805298]
34. Magdelaine-Beuzelin C, Pinault C, Paintaud G, Watier H. Therapeutic antibodies in ophthalmology: Old is new again. *MAbs*. 2010; 2:176–180. [PubMed: 21358858]
35. Miner JJ, et al. Zika Virus Infection during Pregnancy in Mice Causes Placental Damage and Fetal Demise. *Cell*. 2016; 165:1081–1091. [PubMed: 27180225]
36. Cugola FR, et al. The Brazilian Zika virus strain causes birth defects in experimental models. *Nature*. 2016; 534
37. Foy BD, et al. Probable Non-Vector-borne Transmission of Zika Virus, Colorado, USA. *Emerg Infect Dis*. 2011; 17:880–882. [PubMed: 21529401]
38. Musso D, et al. Potential sexual transmission of zika virus. *Emerg Infect Dis*. 2015; 21:359–361. [PubMed: 25625872]
39. Russell K, et al. Male-to-Female Sexual Transmission of Zika Virus — United States, January–April 2016. *Clin Infect Dis*. 2016; 64:ciw692.
40. Davidson A, Slavinski S, Komoto K, Rakeman J, Weiss D. Suspected Female-to-Male Sexual Transmission of Zika Virus — New York City, 2016. *MMWR Morb Mortal Wkly Rep*. 2016; 65:716–717. [PubMed: 27442327]
41. Deckard DT, et al. Male-to-Male Sexual Transmission of Zika Virus — Texas, January 2016. *MMWR Morb Mortal Wkly Rep*. 2016; 65:372–374. [PubMed: 27078057]
42. Barzon L, et al. Infection dynamics in a traveller with persistent shedding of Zika virus RNA in semen for six months after returning from Haiti to Italy, January 2016. *Euro Surveill*. 2016; 21
43. Richner JM, et al. Vaccine Mediated Protection Against Zika Virus- Induced Congenital Disease Vaccine Mediated Protection Against Zika Virus-Induced Congenital Disease. *Cell Chao Shan Camila R Fontes*. 2017; 17018:273–283.
44. Sukopulvi-Petty S, et al. Functional Analysis of Antibodies against Dengue Virus Type 4 Reveals Strain-Dependent Epitope Exposure That Impacts Neutralization and Protection. *J Virol*. 2013; 87:8826–8842. [PubMed: 23785205]
45. Mansuy JM, et al. Zika virus: High infectious viral load in semen, a new sexually transmitted pathogen? *Lancet Infect Dis*. 2016; 16:405.
46. Murray KO, et al. Prolonged Detection of Zika Virus in Vaginal Secretions and Whole Blood. *Emerg Infect Dis*. 2017; 23:99–101. [PubMed: 27748649]
47. Zeitlin L, et al. Enhanced potency of a fucose-free monoclonal antibody being developed as an Ebola virus immunoprotectant. *Proc Natl Acad Sci*. 2011; 108:20690–20694. [PubMed: 22143789]
48. DiLillo DJ, Tan GS, Palese P, Ravetch JV. Broadly neutralizing hemagglutinin stalk-specific antibodies require FcγR interactions for protection against influenza virus in vivo. *Nat Med*. 2014; 20:143–151. [PubMed: 24412922]
49. Hiatt A, et al. Glycan variants of a respiratory syncytial virus antibody with enhanced effector function and in vivo efficacy. *Proc Natl Acad Sci U S A*. 2014; 111:5992–7. [PubMed: 24711420]
50. Carroll T, et al. Zika virus preferentially replicates in the female reproductive tract after vaginal inoculation of rhesus macaques. *PLoS Pathog*. 2017; 13:e1006537. [PubMed: 28746373]
51. Halstead SB. Biologic evidence required for zika disease enhancement by dengue antibodies. *Emerg Infect Dis*. 2017; 23:569–573. [PubMed: 28322690]
52. Brien JD, Lazear HM, Diamond MS. Propagation, Quantification, Detection, and Storage of West Nile Virus. *Curr Protoc Microbiol*. 2013:15D.3.1–15D.3.18.
53. Lanciotti RS. Genetic and serologic properties of Zika virus associated with an epidemic, Yap State, Micronesia, 2007. *Emerg Infect Dis*. 2008; 14:1232–1239. [PubMed: 18680646]
54. Hansen DA, Esakky P, Drury A, Lamb L, Moley KH. The Aryl Hydrocarbon Receptor Is Important for Proper Seminiferous Tubule Architecture and Sperm Development in Mice. *Biol Reprod*. 2014; 908:1–12.

55. Goodson SG, Zhang Z, Tsuruta JK, Wang W, O'brien DA. Classification of Mouse Sperm Motility Patterns Using an Automated Multiclass Support Vector Machines Model. *Biol Reprod.* 2011; 84:1207–1215. [PubMed: 21349820]

Author Manuscript

Author Manuscript

Author Manuscript

Author Manuscript

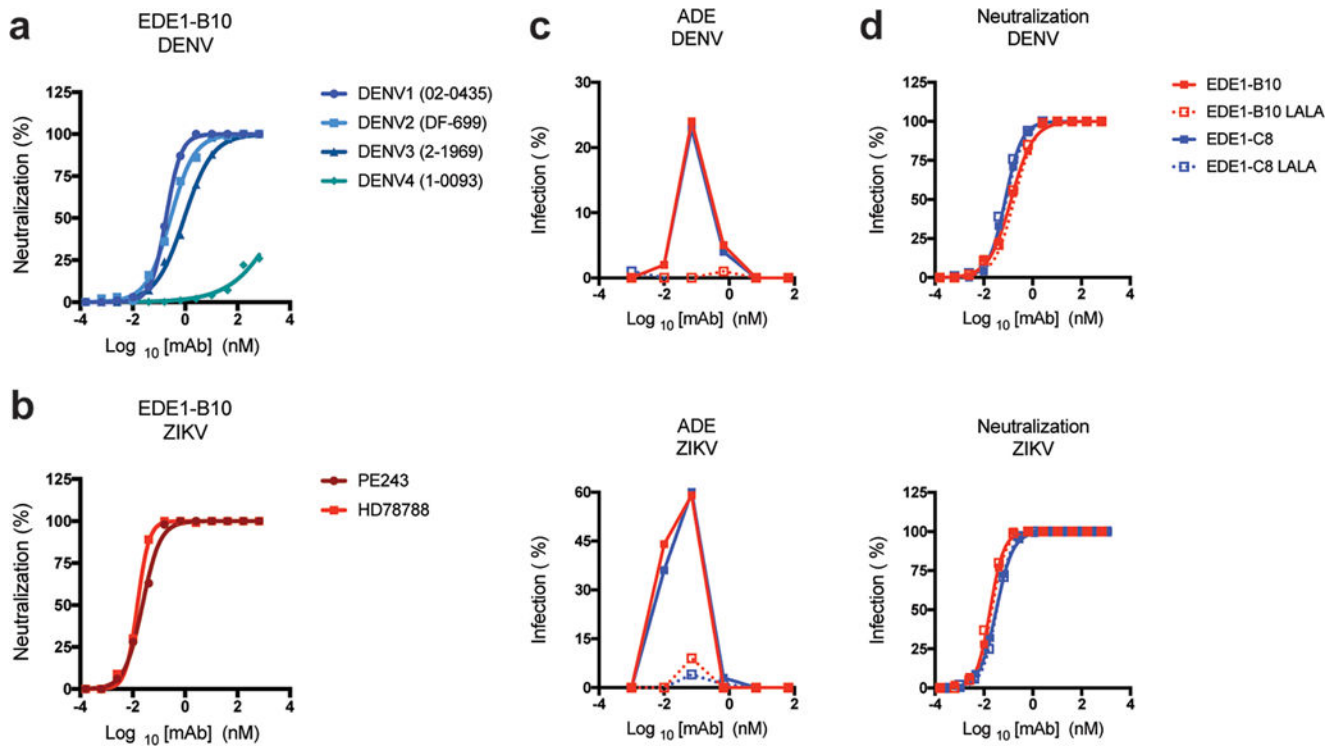
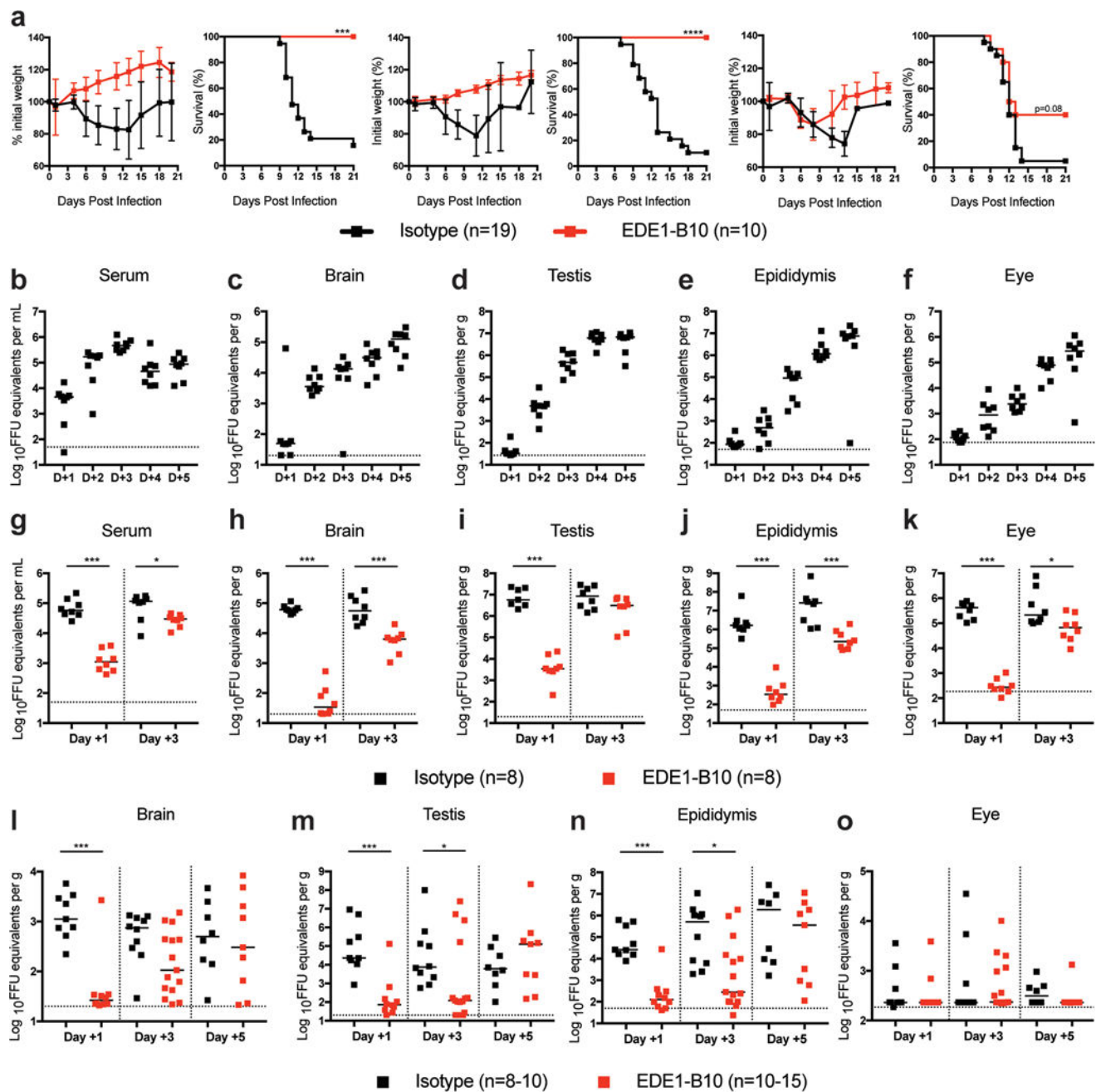


Figure 1.

EDE1-B10 is an anti-DENV human mAb that cross-neutralizes ZIKV infection. **(a)** Serial dilutions of EDE1-B10 were tested for neutralization of DENV-1-4 serotypes using a focus reduction neutralization test. **(b)** EDE1-B10 was tested for neutralization of ZIKV strains from Africa (HD78788) and Brazil (PE243). The data is expressed as the percentage of neutralized virus, and are representative of two to three independent experiments. **(c–d)** ADE **(c)** and neutralization **(d)** studies with wild-type and LALA recombinant variants of EDE1-B10 and EDE1-C8 with DENV-2 (16681) and ZIKV (HD78788). Infection of U937 cells **(c)** in the presence of mAbs EDE1-B10, EDE1-C8, or the LALA mutants is presented as the percentage of infection. Wild-type and LALA EDE1-B10 and EDE1-C8 antibodies exhibited equivalent neutralizing activity **(d)**. Data are representative of three independent experiments.

**Figure 2.**

EDE1-B10 protects against ZIKV induced lethality and viral burden. **a.** Four to five week-old WT male mice were treated with anti-Ifnar1 mAb followed by subcutaneous infection with mouse-adapted ZIKV-Dakar. Mice were then treated with isotype-control mAb or EDE1-B10 at day +1 (100 μ g, left), day +3 (250 μ g, middle), or day +5 (250 μ g, right). Weight and survival data were pooled from two to three independent experiments (isotype, $n = 19$ and EDE1-B10, $n = 10$ per group; ***, $P < 0.001$; ****, $P < 0.0001$; log-rank test). **b-f.** Eight to nine week-old WT male mice were treated with anti-Ifnar1 mAb followed by subcutaneous inoculation with mouse-adapted ZIKV-Dakar. Viral RNA was measured by

qRT-PCR in serum (**b**), brain (**c**), testis (**d**), epididymis (**e**), and eye (**f**). Bars indicate median values from two experimental replicates (n = 8 per group). **g–k**. Eight to nine week-old WT male mice were treated with anti-Ifnar1 mAb followed by subcutaneous inoculation with mouse-adapted ZIKV-Dakar. Mice were treated with isotype-control mAb or EDE1-B10 at day +1 (100 µg) or day +3 (250 µg). At day +5, viral RNA was measured in serum (**g**), brain (**h**), testis (**i**), epididymis (**j**), and eye (**k**). Bars indicate median values collected from two experimental replicates (n = 8 per group). Statistical significance was determined (Mann-Whitney test: *, $P < 0.05$; ***, $P < 0.001$). **i–o**. Eight to nine week-old WT male mice were treated with anti-Ifnar1 mAb followed by subcutaneous inoculation with mouse-adapted ZIKV-Dakar. Mice were treated with isotype control mAb or EDE1-B10 at day +1 (100 µg), day +3 (250 µg), or day +5 (250 µg). At day +21, viral RNA was measured in brain (**l**), testis (**m**), epididymis (**n**), and eye (**o**) tissues. Bars indicate median values collected from three experimental replicates (n = 8–15 per group). Statistical significance was analyzed on all data (Mann-Whitney test: *, $P < 0.05$; ***, $P < 0.001$). Dashed lines indicate the limit of detection of the assay.

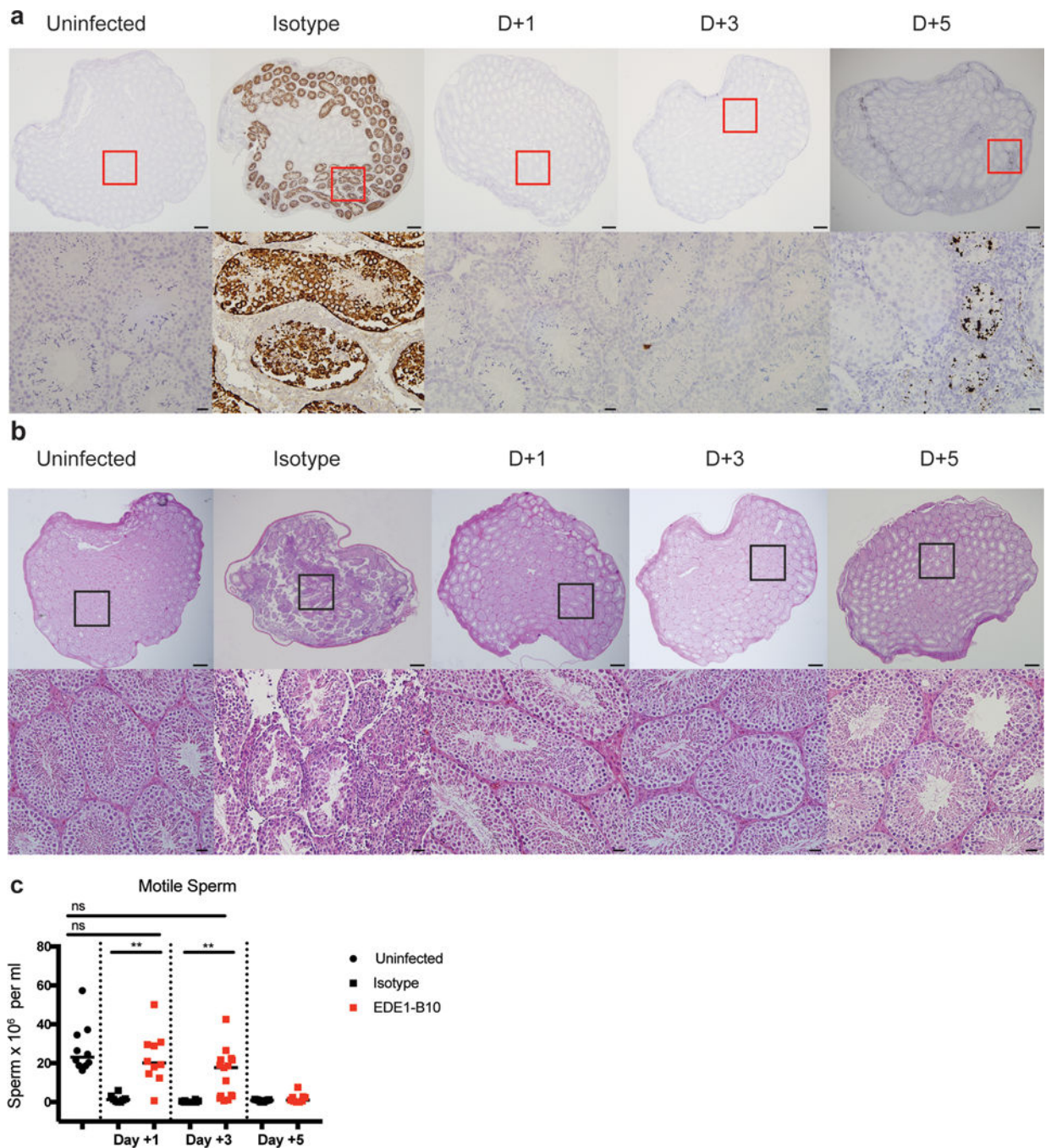


Figure 3.

EDE1-B10 protects against testis infection and injury. Eight to nine week old WT male mice were treated with isotype-control or EDE1-B10 mAb at day +1, +3, or +5 as described in Fig 2. **a.** RNA *in situ* hybridization (ISH) staining of testis at day +21 using ZIKV-specific RNA probes. Low power (scale bar = 500 μ m) and high power (scale bar = 20 μ m) images are presented in sequence. The images are representative of 4 to 6 mice. **b.** Hematoxylin and eosin (H & E) staining of testis. Low power (scale bar = 500 μ m) and high power (scale bar = 20 μ m) images are shown in sequence from mice treated with isotype-control or EDE1-

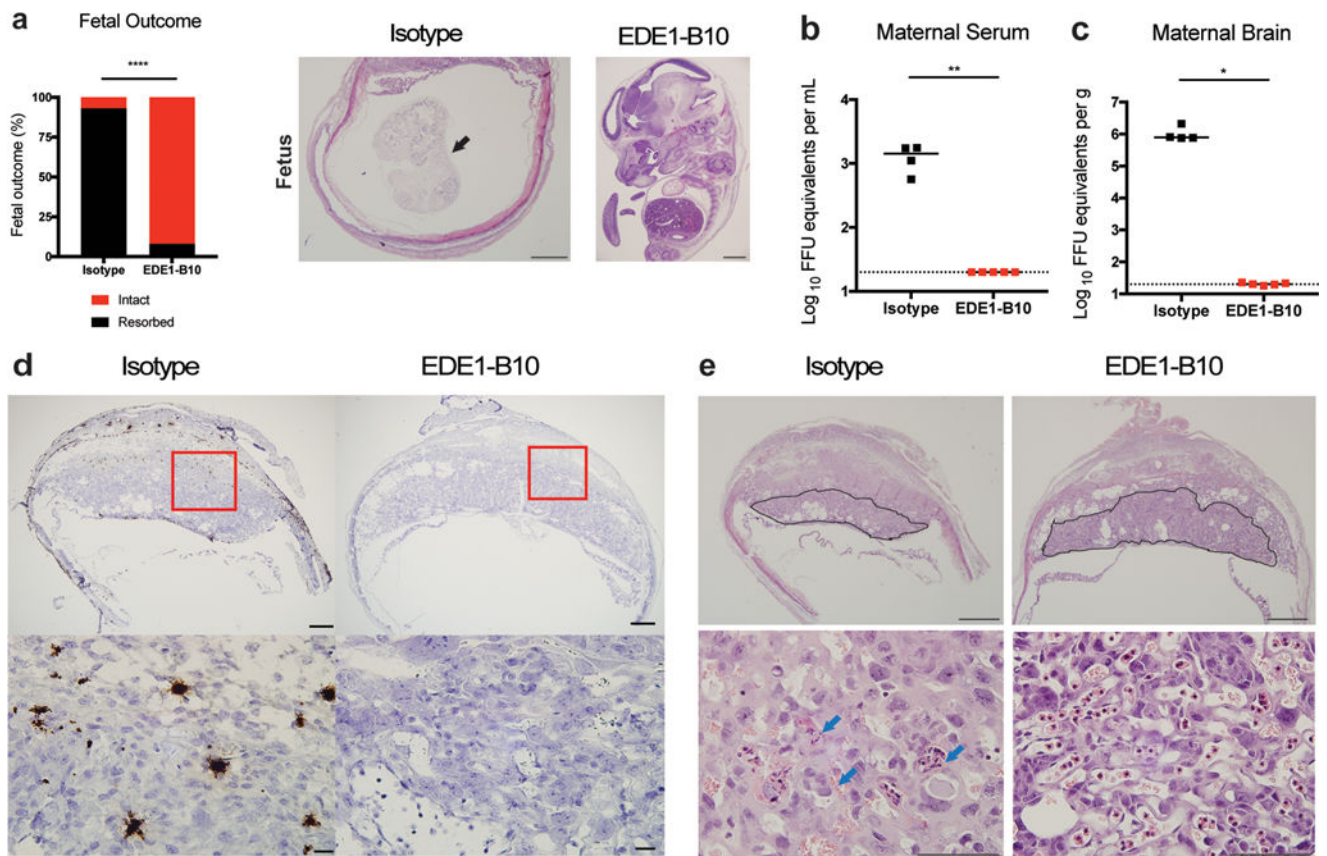
B10 mAbs. The images are representative of testis from 3 to 5 mice. **c.** The number of motile sperm from each mouse was determined by computer assisted sperm analysis. Bars indicate median values of samples collected from three independent experiments ($n = 8-15$ per group). Statistical significance was determined (ANOVA with a Dunn's multiple comparison test: **, $P < 0.01$; ns, not significant).

Author Manuscript

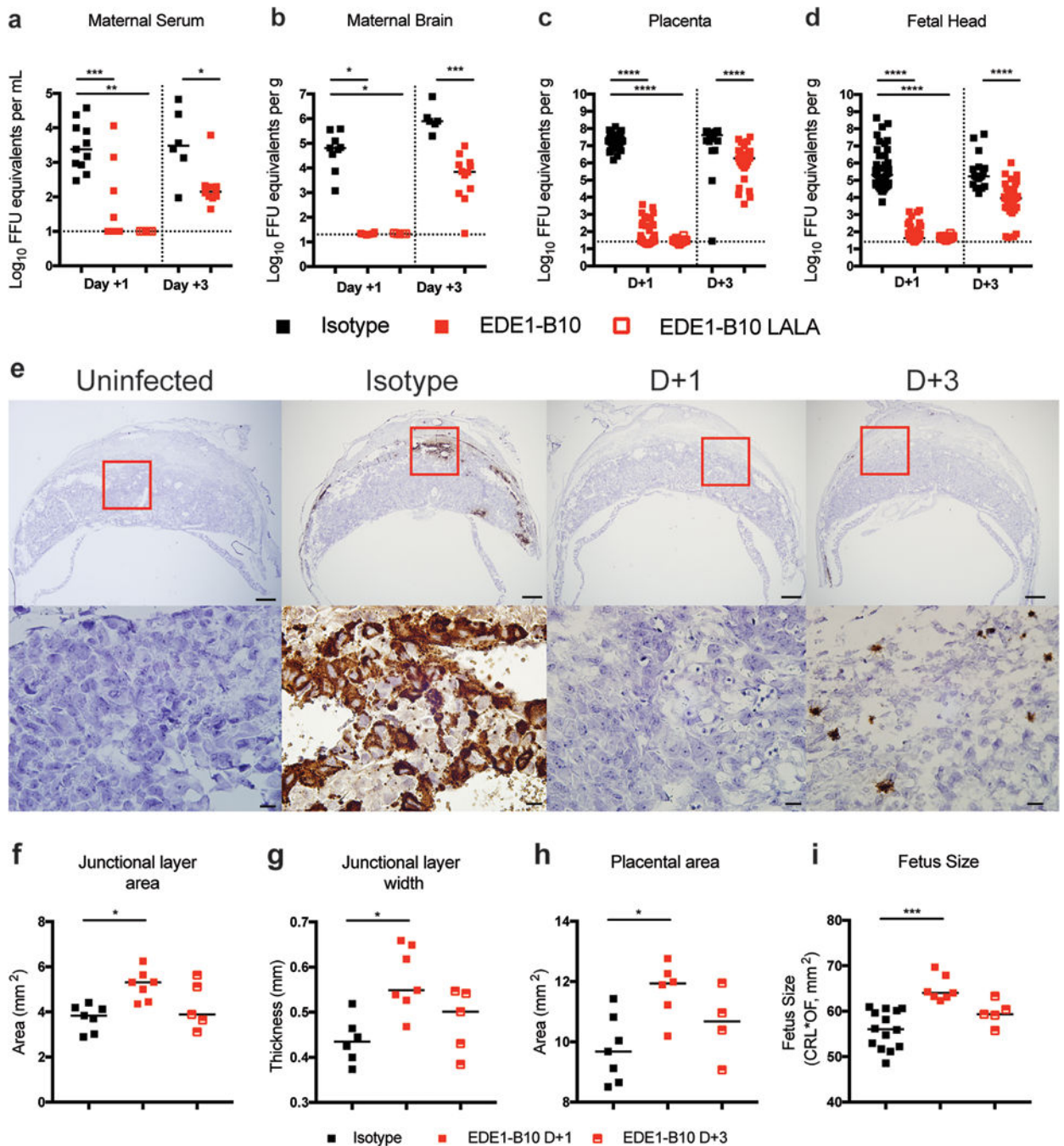
Author Manuscript

Author Manuscript

Author Manuscript

**Figure 4.**

EDE1-B10 protects *Ifnar1*^{-/-} pregnant dams. *Ifnar1*^{-/-} female mice were mated with WT sires. At E6.5, dams were infected with ZIKV-Brazil and treated on E7.5 with 250 µg of isotype-control or EDE1-B10 mAb. Dams were harvested on E13.5 to assess (a) fetal survival and (b and c) maternal viral burden. a. Fetal outcome is presented as intact versus resorbed fetuses at the time of harvest (left panel). Images of fetal histology are shown (right panels). Black arrow indicates a partially resorbed fetus in the uterus (scale bar = 1 mm). b–c. Viral burden in the maternal brain (b) and serum (c). Bars indicates median values. Data were pooled from two independent experiments. Statistical significance for fetal survival was determined by Fisher’s exact test (****, $P < 0.0001$) and viral burden by Mann-Whitney test (*, $P < 0.05$; **, $P < 0.01$). Dashed lines indicates limit of detection for the assay. d. RNA ISH staining of placentas at E13.5. Low power (scale bar = 500 µm) and high power (scale bar = 20 µm) images are presented in sequence. The images are representative of placenta from 2 to 3 dams. e. H & E staining of placenta and fetus at E13.5. Placental labyrinth zone is marked with a solid line. Low power (scale bar = 1 mm) and high power (scale bar = 100 µm) images of placentas are presented in sequence. Blue arrows indicate apoptotic trophoblasts in the labyrinth zone.

**Figure 5.**

Therapeutic effect of EDE1-B10 in WT pregnant dams. WT female mice were mated with WT sires. At E5.5, dams were treated with anti-Ifnar1 mAb. At E6.5, dams were infected subcutaneously with 10^3 FFU of mouse-adapted ZIKV-Dakar. At E7.5 (day +1) or E9.5 (day +3), dams were treated with 250 μ g of either isotype-control, EDE1-B10, or EDE1-B10 LALA mAbs. At E13.5, maternal serum (**a**), maternal brain (**b**), placenta (**c**), and fetal head (**d**) were harvested, and viral RNA was assessed by qRT-PCR. Bars indicate median values. Data was pooled from 3 to 5 independent experiments. Statistical significance was

determined by Kruskal-Wallis or Holm-Sidak's multiple comparisons test (D+1 samples) or Mann-Whitney test (D+3 samples) (*, $P < 0.05$; **, $P < 0.01$; ***, $P < 0.001$; ****, $P < 0.0001$). Dashed lines indicate the limit of detection for the assay. **e.** RNA ISH staining of placenta at E13.5. Low power (scale bar = 500 μm) and high power (scale bar = 20 μm) images are shown in sequence. The images are representative of placenta from 4 to 5 dams. **f-i** Measurements of the placenta (**f-h**) and fetus body size (**i**). Bars indicate median values. Significance was analyzed by Kruskal-Wallis test with a Dunn's multiple comparison test (*, $P < 0.05$; **, $P < 0.01$)

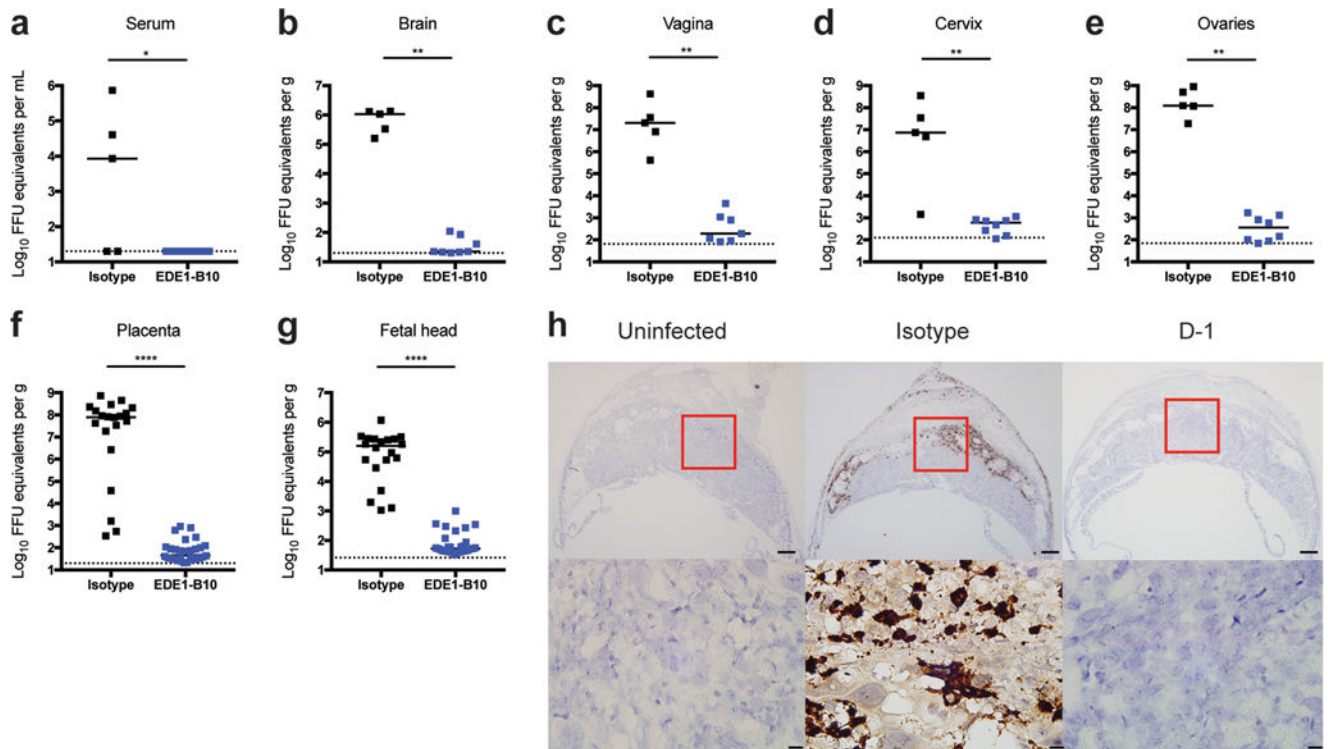


Figure 6. EDE1-B10 prevents maternal and fetal ZIKV infection after intravaginal inoculation of pregnant dams. WT female mice were mated with WT sires. At E5.5 (day -1), dams were treated with anti-Ifnar1 mAb and a single 250 μ g dose of either isotype-control mAb or EDE1-B10. At E6.5, dams were inoculated intravaginally with 10^5 FFU mouse-adapted ZIKV-Dakar. At E13.5, maternal serum (**a**), maternal brain (**b**), vagina (**c**), cervix (**d**), ovary (**e**), placenta (**f**), and fetal head (**g**) were harvested, and viral RNA was assessed by qRT-PCR. Bars indicate median values. Data was pooled from three independent experiments. Statistical significance was determined by Mann-Whitney test (*, $P < 0.05$; **, $P < 0.01$; ***, $P < 0.001$; ****, $P < 0.0001$). Dashed line indicates limit of detection for the assay. **h.** RNA ISH staining of placenta at E13.5. Low power (scale bar = 500 μ m) and high power (scale bar = 20 μ m) images are presented. The images in panels are representative of placentas from 3 to 4 dams.